Acta Crystallographica Section C
Crystal Structure Communications
ISSN 0108-2701

Synthetic ferric sulfate trihydrate, $Fe_2(SO_4)_3\cdot 3H_2O$, a new ferric sulfate salt

Wenqian Xu[a]* and John B. Parise[b]

[a]Department of Geosciences, Stony Brook University, Stony Brook, NY 11794-2100, USA, and [b]Department of Geosciences and Department of Chemistry, Stony Brook University, Stony Brook, NY 11794-2100, USA
Correspondence e-mail: wenqian.xu@stonybrook.edu

Received 9 February 2011
Accepted 2 April 2011
Online 13 April 2011

Ferric sulfate trihydrate has been synthesized at 403 K under hydrothermal conditions. The structure consists of quadruple chains of $[Fe_2(SO_4)_3(H_2O)_3]^0_\infty$ parallel to [010]. Each quadruple chain is composed of equal proportions of $FeO_4(H_2O)_2$ octahedra and $FeO_5(H_2O)$ octahedra sharing corners with SO_4 tetrahedra. The chains are joined to each other by hydrogen bonds. This compound is a new hydration state of $Fe_2(SO_4)_3\cdot nH_2O$; minerals with n = 0, 5, 7.25–7.75, 9 and 11 are found in nature.

Comment

Ferric sulfate trihydrate belongs to a group of ferric sulfates sharing the general formula $Fe_2(SO_4)_3\cdot nH_2O$, which includes mikasaite (n = 0; Miura *et al.*, 1994), lausenite (n = 5; Majzlan *et al.*, 2005), kornelite (n = 7.25–7.75; Ackermann *et al.*, 2009; Robinson & Fang, 1973), paracoquimbite (n = 9; Robinson & Fang, 1971), quenstedtite (n = 11; Thomas *et al.*, 1974) and a synthetic $Fe_2(SO_4)_3$ (n = 0), which is a polymorph of mikasaite (Christidis & Rentzeperis, 1975). These ferric sulfate minerals are usually found as efflorescence in acid mine drainage (AMD) areas, formed as oxidation products of pyrite (FeS_2) and other sulfide minerals (Jambor *et al.*, 2000). Other commonly found ferric sulfates in AMD regions include coquimbite $[(Fe,Al)_2(SO_4)_3\cdot 9H_2O]$, jarosite $[KFe_3(SO_4)_2(OH)]$, rhomboclase $[(H_5O_2)Fe(SO_4)_2\cdot 2H_2O]$ and copiapite $[Fe^{2+}Fe^{3+}_4(SO_4)_2(OH)_2\cdot 20H_2O]$. Dissolution of these minerals greatly increases water acidity because of ferric ion hydrolysis. Plus, these ferric sulfates usually absorb or co-precipitate with toxic metals such as Cr and Pb, and act as a secondary source of these toxic metal pollutants in local waters as they dissolve (Jambor *et al.*, 2000). To better control and reduce the adverse environmental effects of ferric sulfates require a thorough understanding of the behavior and stability of these minerals as functions of environmental factors, such as pH, relative humidity and temperature. Understanding the transformations of the ferric sulfates as a function of environmental conditions has been the focus of recent studies (Ackermann *et al.*, 2009; Majzlan, 2010; Tosca *et al.*, 2007; Xu *et al.*, 2009, 2010).

One difficulty in delineating phase stability relationships in the Fe^{III}–SO_4–H_2O system is the need for correct and complete crystal structure models for all phases in the system. For example, paracoquimbite and coquimbite had for a long time been considered as polymorphs (Fang & Robinson, 1970) until a recent study showing the amount of aluminium in the mineral determines the structure type: paracoquimbite is pure $Fe_2(SO_4)_3\cdot 9H_2O$, while coquimbite has an Al/Fe ratio close to 1:3, with Al predominantly occupying the $[M(H_2O)_6]^{3+}$ metal site (Majzlan *et al.*, 2010). A third structure type in this coquimbite series was recently found in a mineral with a 1:1 Al/Fe ratio (Demartin *et al.*, 2010). Further, the synthesis of ferric sulfates often produces new phases (Chipera *et al.*, 2007; Freeman *et al.*, 2009; Majzlan *et al.*, 2005; Peterson *et al.*, 2009; Xu *et al.*, 2009). Structures of these new phases are mostly unresolved because of their occurrence only as fine-grained mixed-phase powders. During the course of our survey of the Fe^{III}–SO_4–H_2O system, we discovered a new phase, namely ferric sulfate trihydrate, $Fe_2(SO_4)_3\cdot 3H_2O$.

The structure of the trihydrate contains identical quadruple chains of $[Fe_2(SO_4)_3(H_2O)_3]^0_\infty$ parallel to [010], as shown in Fig. 1. Each quadruple chain consists of four single chains of alternating FeO_6 octahedra and SO_4 tetrahedra extending along the b axis. Of the four single chains, two are symmetrically independent as '–Fe1–S1–Fe1–' and '–Fe2–S2–Fe2–'; the other two are generated through an inversion center. A third sulfate group $S3O_4$ connects to $Fe1O_6$ and $Fe2O_6$ by corner sharing. Of the three unique water molecules, one (O1*W*) is coordinated to the Fe1 site, and the other two (O2*W* and O3*W*) are coordinated to the Fe2 site.

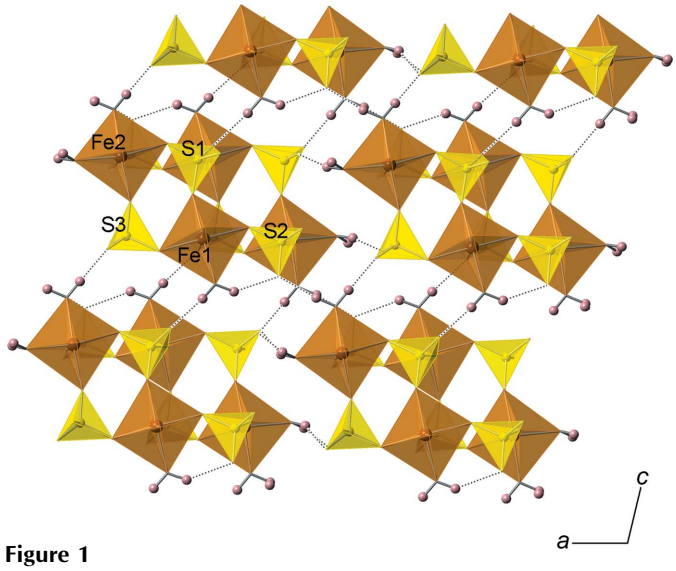

Figure 1
The ferric sulfate trihydrate structure, viewed down the b axis. FeO_6 octahedra are dark (brown in the electronic version of the paper), SO_4 tetrahedra are light (yellow) and H atoms are small spheres. Dotted lines denote hydrogen bonds. Atom labels are generic and do not correspond exactly to the asymmetric unit defined in the CIF.

  doi:10.1107/S0108270111012273

The quadruple chains are linked to one another by water–sulfate O—H···O hydrogen bonds (Table 2). All hydrogen bonds involve the terminal O atoms of SO_4 groups as the acceptor, except the O1*W*—H1*B*···O3^{iv} [symmetry code: (iv) $-x, y-\frac{1}{2}, -z+\frac{1}{2}$] hydrogen bond, where the acceptor O atom bridges Fe1 and S1. There is also one intramolecular hydrogen bond, *viz.* O1*W*—H1*B*···O8.

The quadruple chain structure of ferric sulfate trihydrate has no similar counterparts in any known sulfates. Though unique, the trihydrate structure shares similarities with other phases in the $Fe_2(SO_4)_3{\cdot}nH_2O$ group. For example, the FeO_6 octahedra do not directly connect with each other but are linked *via* corner-sharing SO_4 tetrahedra. It should be mentioned that FeO_6 octahedra do share corners in some other ferric sulfates such as copiapite and jarosite.

Including the trihydrate described here, there are a total of six hydration states of $Fe_2(SO_4)_3{\cdot}nH_2O$; namely n = 0, 3, 5, 7.25–7.75, 9 and 11. Anhydrous ferric sulfate has two polymorphs, a monoclinic form and a trigonal form. The trigonal form occurs in nature as the mineral mikasaite, while the synthetic monoclinic form has no mineral equivalent (Christidis & Rentzeperis, 1975; Miura *et al.*, 1994). Both forms consist of frameworks of connected FeO_6 octahedra and SO_4 tetrahedra. The structure of lausenite, $Fe_2(SO_4)_3{\cdot}5H_2O$, is composed of corrugated slabs of $[Fe_2(SO_4)_3(H_2O)_5]^0_\infty$ (Majzlan *et al.*, 2005). The five water molecules shown in the formula are all coordinated to the two Fe sites, two coordinated to one and three coordinated to the other. The structure of kornelite, $Fe_2(SO_4)_3{\cdot}7.25$–$7.75H_2O$, consists of slabs similar to those in lausenite, with a formula $[Fe_2(SO_4)_3(H_2O)_6]^0_\infty$. Each of the two Fe sites is bonded to three water molecules. The remaining 1.25 to 1.75 water molecules shown in the formula are located between neighboring slabs as isolated water (Robinson & Fang, 1973). The paracoquimbite structure contains isolated clusters of $[Fe(H_2O)_6]^{3+}$ and $[Fe_3(SO_4)_6(H_2O)_6]^{3-}$, together with six uncoordinated water molecules (Robinson & Fang, 1971). The structure of quenstedtite, $Fe_2(SO_4)_3{\cdot}11H_2O$, consists of isolated clusters of $[Fe(SO_4)(H_2O)_5]^+$ and $[Fe(SO_4)_2(H_2O)_4]^-$, together with two uncoordinated water molecules (Thomas *et al.*, 1974).

As the hydration state increases, FeO_6 octahedra and SO_4 tetrahedra tend to be disassociated, as more water molecules coordinate to Fe to form simple clusters. The hydration state of the trihydrate lies between that of anhydrous ferric sulfate and lausenite. Like lausenite, the structure of the trihydrate does not have uncoordinated water molecules as found in kornelite and higher hydration states. As opposed to limited clusters in the higher hydration states, both the trihydrate and lausenite have infinite clusters, *viz.* one-dimensional chains for the trihydrate and two-dimensional slabs for lausenite. Further, the quadruple chain of the trihydrate has three terminal O-atom sites for water molecules, while the slab of lausenite has five. This appears to be counterintuitive: a common first impression would be that a chain arrangement has more terminal O-atom sites than two-dimensional sheets. It is easy to understand this if one considers the fact that a quadruple chain has far fewer terminal sites than four single chains; also, the slab in lausenite is less like a dense sheet such as the MnO_2 layer in birnessite, and closer to a net of interlaced chains.

Therefore, the trihydrate, though having a unique quadruple chain structure, shares the basic structural features present in other phases in the $Fe_2(SO_4)_3{\cdot}nH_2O$ system. The trihydrate structure also fits in the trend of structural changes set by hydration levels.

Experimental

α-Fe_2O_3 [1.000 (1) g] and sulfuric acid [1.939 (1) g] with a nominal concentration of 95.9 wt% H_2SO_4 were mixed in a 23 ml Teflon-lined vessel, sealed in a Parr stainless steel autoclave and then stored in an isotemp oven set at 403 K for 9 d. The product was an inhomogeneous yellow–pink solid block. Examination with optical microscopy revealed transparent yellow crystals embedded in a pink powdery matrix. The yellow crystals are cuboids or short rectangular prisms, 100 to 300 µm on the longest edge and 40 to 100 µm on the shortest edge. The structure of the yellow crystal was determined from single-crystal X-ray diffraction to be the title ferric sulfate trihydrate. The pink matrix was a combination of lausenite and rhomboclase identified from powder X-ray diffraction (see *Supplementary material*).

Crystal data

$Fe_2(SO_4)_3{\cdot}3H_2O$
M_r = 453.93
Monoclinic, $P2_1/c$
a = 11.281 (3) Å
b = 6.336 (2) Å
c = 16.278 (5) Å
β = 102.676 (8)°
V = 1135.1 (6) Å^3
Z = 4
Mo $K\alpha$ radiation
μ = 3.20 mm^{-1}
T = 298 K
0.12 × 0.12 × 0.06 mm

Data collection

Bruker SMART CCD diffractometer
Absorption correction: multi-scan (*SADABS*; Bruker, 2001)
T_{min} = 0.700, T_{max} = 0.831
7266 measured reflections
2309 independent reflections
1894 reflections with $I > 2\sigma(I)$
R_{int} = 0.033

Refinement

$R[F^2 > 2\sigma(F^2)]$ = 0.028
$wR(F^2)$ = 0.084
S = 1.05
2309 reflections
199 parameters
6 restraints
H atoms treated by a mixture of independent and constrained refinement
$\Delta\rho_{max}$ = 0.49 e Å^{-3}
$\Delta\rho_{min}$ = −0.55 e Å^{-3}

H atoms were found in difference Fourier maps and subsequently placed in idealized positions with restrained O—H distances of 0.90 (3) Å, and with U_{iso}(H) = 1.2U_{iso}(O).

Data collection: *SMART* (Bruker, 1998); cell refinement: *SAINT-Plus* (Bruker, 1998); data reduction: *SAINT-Plus*; program(s) used to solve structure: *SHELXS97* (Sheldrick, 2008); program(s) used to refine structure: *SHELXL97* (Sheldrick, 2008); molecular graphics: *CrystalMaker* (Palmer, 2010); software used to prepare material for publication: *SHELXL97*.

The synthesis of ferric sulfates at Stony Brook by Wenqian Xu was supported by NASA grant No. MFRP07-0022 (JBP). The single-crystal diffractometer and software used to deter-

Table 1
Selected geometric parameters (Å, °).

Fe1—O9^{i}	1.932 (2)	Fe2—O10	1.941 (2)
Fe1—O2^{i}	1.9814 (19)	Fe2—O7	1.993 (2)
Fe1—O5	1.984 (2)	Fe2—O2*W*	1.997 (2)
Fe1—O4^{ii}	2.0142 (19)	Fe2—O3*W*	1.998 (2)
Fe1—O1*W*	2.016 (2)	Fe2—O6^{iii}	2.008 (2)
Fe1—O3	2.0553 (19)	Fe2—O1	2.023 (2)
O9^{i}—Fe1—O2^{i}	93.77 (8)	O5—Fe1—O1*W*	90.88 (9)
O9^{i}—Fe1—O5	178.31 (8)	O4^{ii}—Fe1—O1*W*	92.23 (8)
O2^{i}—Fe1—O5	87.50 (8)	O9^{i}—Fe1—O3	87.92 (7)
O9^{i}—Fe1—O4^{ii}	88.33 (7)	O2^{i}—Fe1—O3	88.11 (7)
O2^{i}—Fe1—O4^{ii}	90.58 (8)	O5—Fe1—O3	91.02 (7)
O5—Fe1—O4^{ii}	92.76 (7)	O4^{ii}—Fe1—O3	175.94 (8)
O9^{i}—Fe1—O1*W*	87.80 (9)	O1*W*—Fe1—O3	89.18 (8)
O2^{i}—Fe1—O1*W*	176.82 (8)		

Symmetry codes: (i) $-x, -y+1, -z$; (ii) $x, y-1, z$; (iii) $x, y+1, z$.

mine the trihydrate structure were funded by grant No. NSF-DMR-0800415 (JBP).

Supplementary data for this paper are available from the IUCr electronic archives (Reference: QS3002). Services for accessing these data are described at the back of the journal.

References

Ackermann, S., Lazic, B., Armbruster, T., Doyle, S., Grevel, K. D. & Majzlan, J. (2009). *Am. Mineral.* **94**, 1620–1628.

Bruker (1998). *SMART* and *SAINT-Plus*. Bruker AXS Inc., Madison, Wisconsin, USA.

Bruker (2001). *SADABS*. Bruker AXS Inc., Madison, Wisconsin, USA.

Chipera, S. J., Vaniman, D. T. & Bish, D. L. (2007). Lunar and Planetary Science Conference XXXVIII, March 12–16, League City, Texas. Abstract No. 1409.

Christidis, P. C. & Rentzeperis, P. J. (1975). *Z. Kristallogr.* **141**, 233–245.

Table 2
Hydrogen-bond geometry (Å, °).

D—H···*A*	*D*—H	H···*A*	*D*···*A*	*D*—H···*A*
O1*W*—H1*A*···O8	0.85 (2)	2.05 (3)	2.754 (3)	140 (3)
O1*W*—H1*B*···O3^{iv}	0.87 (2)	2.05 (2)	2.907 (3)	173 (3)
O2*W*—H2*A*···O12^{v}	0.91 (2)	1.76 (2)	2.655 (3)	166 (3)
O2*W*—H2*B*···O11^{vi}	0.87 (2)	2.01 (2)	2.837 (3)	157 (3)
O3*W*—H3*A*···O8^{vii}	0.88 (2)	1.81 (2)	2.677 (3)	171 (3)
O3*W*—H3*B*···O11^{viii}	0.88 (2)	1.81 (2)	2.676 (3)	171 (3)

Symmetry codes: (iv) $-x, y-\frac{1}{2}, -z+\frac{1}{2}$; (v) $-x+1, -y+1, -z$; (vi) $-x+1, -y+2, -z$; (vii) $-x+1, y+\frac{1}{2}, -z+\frac{1}{2}$; (viii) $x, -y+\frac{3}{2}, z+\frac{1}{2}$.

Demartin, F., Castellano, C., Gramaccioli, C. M. & Campostrini, I. (2010). *Can. Mineral.* **48**, 323–333.

Fang, J. H. & Robinson, P. D. (1970). *Am. Mineral.* **55**, 1534–1540.

Freeman, J. J., Wang, A. & Ling, Z. C. (2009). Lunar and Planetary Science Conference XXXX, March 23–27, Houston, Texas. Abstract No. 2284.

Jambor, J. I., Nordstrom, D. K. & Alpers, C. N. (2000). *Metal–Sulfate Salts from Sulfide Mineral Oxidation*. Washington, DC: Mineralogical Society of America, Geochemical Society.

Majzlan, J. (2010). *Chimia*, **64**, 699–704.

Majzlan, J., Botez, C. & Stephens, P. W. (2005). *Am. Mineral.* **90**, 411–416.

Majzlan, J., Dordevic, T., Kolitsch, U. & Schefer, J. (2010). *Mineral. Petrol.* **100**, 241–248.

Miura, H., Niida, K. & Hirama, T. (1994). *Mineral. Mag.* **58**, 649–653.

Palmer, D. (2010). *CrystalMaker*. CrystalMaker Software Ltd, Yarnton, Oxfordshire, England.

Peterson, R. C., Valyashko, E. & Wang, R. Y. (2009). *Can. Mineral.* **47**, 625–634.

Robinson, P. D. & Fang, J. H. (1971). *Am. Mineral.* **56**, 1567–1572.

Robinson, P. D. & Fang, J. H. (1973). *Am. Mineral.* **58**, 535–539.

Sheldrick, G. M. (2008). *Acta Cryst.* A**64**, 112–122.

Thomas, J. N., Robinson, P. D. & Fang, J. H. (1974). *Am. Mineral.* **59**, 582–586.

Tosca, N. J., Smirnov, A. & McLennan, S. M. (2007). *Geochim. Cosmochim. Acta*, **71**, 2680–2698.

Xu, W. Q., Parise, J. B. & Hanson, J. (2010). *Am. Mineral.* **95**, 1408–1412.

Xu, W. Q., Tosca, N. J., McLennan, S. M. & Parise, J. B. (2009). *Am. Mineral.* **94**, 1629–1637.